

Coupled valence and spin state transition in $(\text{Pr}_{0.7}\text{Sm}_{0.3})_{0.7}\text{Ca}_{0.3}\text{CoO}_3$

F. Guillou,¹ Q. Zhang,¹ Z. Hu,² C. Y. Kuo,² Y. Y. Chin,³ H. J. Lin,³ C. T. Chen,³ A. Tanaka,⁴ L. H. Tjeng,² and V. Hardy¹

¹Laboratoire CRISMAT, ENSICAEN, UMR 6508 CNRS, 6 Boulevard du Maréchal Juin, 14050 Caen Cedex, France

²Max Planck Institute for Chemical Physics of Solids, Nöthnitzer Straße 40, 01187 Dresden, Germany

³National Synchrotron Radiation Research Center (NSRRC), 101 Hsin-Ann Road, Hsinchu 30077, Taiwan

⁴Department of Quantum Matters, ADSM, Hiroshima University, Higashi-Hiroshima, 739-8530, Japan

(Received 21 December 2012; published 11 March 2013)

The coupled valence and spin state transition (VSST) taking place in $(\text{Pr}_{0.7}\text{Sm}_{0.3})_{0.7}\text{Ca}_{0.3}\text{CoO}_3$ was investigated by soft x-ray absorption spectroscopy (XAS) experiments carried out at the Pr- $M_{4,5}$, Co- $L_{2,3}$, and O- $1s$ edges. This VSST is found to be composed of a sharp Pr/Co valence and Co spin state transition centered at $T^* \sim 89.3$ K, followed by a smoother Co spin-state evolution at higher temperatures. At $T < T^*$, we found that the praseodymium displays a mixed valence $\text{Pr}^{3+}/\text{Pr}^{4+}$ with about 0.13 $\text{Pr}^{4+}/\text{f.u.}$, while all the Co^{3+} is in the low-spin (LS) state. At $T \sim T^*$, the sharp valence transition converts all the Pr^{4+} to Pr^{3+} with a corresponding Co^{3+} to Co^{4+} compensation. This is accompanied by an equally sharp spin state transition of the Co^{3+} from the low to an incoherent mixture of low and high-spin (HS) states. An involvement of the intermediate-spin (IS) state can be discarded for the Co^{3+} . While above T^* and at high temperatures the system shares rather similar properties as Sr-doped LaCoO_3 , at low temperatures, it behaves much more like EuCoO_3 with its highly stable LS configuration for the Co^{3+} . Apparently, the mechanism responsible for the formation of Pr^{4+} at low temperatures also helps to stabilize the Co^{3+} in the LS configuration despite the presence of Co^{4+} ions. We also found out that that the Co^{4+} is in an IS state over the entire temperature range investigated in this study (10–290 K). The presence of Co^{3+} HS and Co^{4+} IS at elevated temperatures facilitates the conductivity of the material.

DOI: [10.1103/PhysRevB.87.115114](https://doi.org/10.1103/PhysRevB.87.115114)

PACS number(s): 71.30.+h, 71.70.-d, 75.47.Lx, 78.70.Dm

I. INTRODUCTION

For some transition-metal ions placed in certain ligand field symmetries, the two main energy terms acting on the intra-atomic electronic configuration (i.e., the crystal-field splitting Δ_{CF} and the Hund exchange J_H) turn out to be very close to each other. This can result in the stabilization of different electronic configurations, as well as the occurrence of transitions between them, induced by temperature or external stimuli like pressure or light irradiation. In condensed matter, such a peculiar situation is most often encountered for $3d^5$ and $3d^6$ cations in a cubicle environment.

The spin state transitions (SST) are among the most intriguing phenomena in solid state physics, and they have been the subject of continuing interest since more than fifty years. In oxides, the cation most prone to such a behavior is Co^{3+} ($3d^6$) located at an octahedral site, which can exhibit not only low-spin (LS) and high-spin (HS) states (corresponding to $t_{2g}^6 e_g^0$ and $t_{2g}^4 e_g^2$, respectively), but also the so-called intermediate-spin state (IS), when the ligand hole state is important (formally noted $t_{2g}^5 e_g^1$, even though it is expected to be a highly hybridized state).¹⁻³

To investigate the SST associated to Co^{3+} , the archetypical material, which has been intensively studied since the 1950s, is the perovskite LaCoO_3 .⁴⁻⁷ It exhibits two broad transitions, one located around $T_1 \sim 100$ K and the second around $T_2 \sim 500$ K. In spite of a huge amount of experimental and theoretical works, there is no consensus about the nature of the Co^{3+} spin states associated to these transitions.⁸⁻¹³ Regarding T_1 for instance, there is still an intense debate in which the two most often investigated pictures involve a transition from an LS state at low temperature to either an IS state^{8,14,15} or a mixed LS/HS state.^{10,11,13,16} Even though the

former scenario is the prevailing one nowadays, some authors strongly dispute it and even question the possibility of an IS state for Co^{3+} in LaCoO_3 .¹¹ It must be emphasized that the thermally driven transitions in LaCoO_3 are quite smooth, rather looking like crossovers associated with gradual populations of excited states, a feature that adds a degree of complexity in all interpretations.

In 2002, Tsubouchi *et al.* reported in $\text{Pr}_{0.5}\text{Ca}_{0.5}\text{CoO}_3$ another type of SST,¹⁷ which is much sharper, located at a characteristic temperature that is hereafter referred to as T^* . It was found that the transition taking place at $T^* \sim 90$ K in $\text{Pr}_{0.5}\text{Ca}_{0.5}\text{CoO}_3$ is actually a first-order transition, associated to discontinuous changes in various physical quantities like magnetization, entropy, and resistivity. As compared to LaCoO_3 , another basic difference is that $\text{Pr}_{0.5}\text{Ca}_{0.5}\text{CoO}_3$ is a mixed valence compound (0.5 Co^{3+} and 0.5 Co^{4+} per formula unit when considering Pr^{3+} and Ca^{2+}). It thus deserves to be noted that Co^{4+} ($3d^5$) sitting at an octahedral site is also susceptible to take different spin states. One could even add that, in the original paper reporting on the possibility of IS states in cobalt oxides, the occurrence of such a state was claimed to be more favorable for Co^{4+} than for Co^{3+} .¹ Soon after the discovery of an SST in $\text{Pr}_{0.5}\text{Ca}_{0.5}\text{CoO}_3$, there was a systematic investigation of perovskite compounds (ABO_3), with Co at the octahedral B site and various combinations of rare-earth and alkaline-earth elements at the A site. It was found that a sharp SST can take place over a quite wide range of composition, which, however, appeared to always require the presence of Pr and Ca on the A site of the perovskite, leading to the formulation $(\text{Pr}_{1-y}\text{Ln}_y)_{1-x}\text{Ca}_x\text{CoO}_3$.¹⁸⁻²⁴

The interpretation of the SST at T^* initially given by Tsubouchi *et al.* was to consider a transition from Co^{3+} LS to Co^{3+} IS upon warming, while Co^{4+} stay in an LS state at all

temperatures.^{17,19} Starting from 2010, however, an accumulation of data pointed to a more complex scenario, involving a valence transition in praseodymium. First, in a neutron powder diffraction study of $\text{Pr}_{0.5}\text{Ca}_{0.5}\text{CoO}_3$, Barón-González *et al.*²⁵ observed that the Co-O bonds are almost unaltered at T^* , whereas the Pr-O ones change a lot, a result leading them to suggest the possibility of a charge transfer between Co and Pr at the transition. This viewpoint was supported soon after by electronic structure calculations performed by Knížek *et al.*,²⁶ who reported a partial change from $(\text{Pr}^{4+}/\text{Co}^{3+})$ below T^* to $(\text{Pr}^{3+}/\text{Co}^{4+})$ above T^* . Then, analyzing heat capacity data in $(\text{Pr}_{1-y}\text{Y}_y)_{0.7}\text{Ca}_{0.3}\text{CoO}_3$ compounds, Hejtmánek *et al.*²⁷ found a Schottky-like anomaly at $T < T^*$, a feature strongly suggesting the presence of the Kramers ion Pr^{4+} ($4f^1$). Finally, in 2011, experiments using soft x-ray absorption spectroscopy (XAS) provided direct evidences of the presence of Pr^{4+} below T^* . In $\text{Pr}_{0.5}\text{Ca}_{0.5}\text{CoO}_3$, García-Muñoz *et al.*²⁸ and Herrero-Martín *et al.*²⁹ both demonstrated a partial oxidation of Pr^{3+} into Pr^{4+} when crossing T^* upon cooling. The quantitative estimate of the fraction of Pr^{4+} at $T \ll T^*$, however, was found to vary between 0.075 and 0.13 $\text{Pr}^{4+}/\text{f.u.}$ ^{28,29} Moreover, it was emphasized that this phenomenon is more complex than a simple valence change, since it also involves the development of a strong hybridization between Pr $4f$ and O $2p$ orbitals below T^* .²⁹

The most generally accepted scheme for the valence and spin state transition (VSST) discussed above is the following:^{17,19,21,22,24} below T^* , a fraction of Pr is in a nominal Pr^{4+} state, the rest being in the more usual Pr^{3+} state; both the Co^{3+} and Co^{4+} are in an LS state; when crossing T^* upon warming, Pr^{4+} transform to Pr^{3+} , this being counterbalanced by a concomitant increase of the Co^{4+} content at the expense of the Co^{3+} one; in terms of spin state, the Co^{3+} LS transform to IS while the Co^{4+} remain in an LS state. While the existence of a valence change involving Pr at the transition is well documented now, the nature of the Co spin states below and above the transition remains a matter of debate. As a matter of act, a very recent work favored the transition towards LS/HS for Co^{3+} above T^* , but it did not categorically rule out the IS scenario.³⁰ Moreover, we emphasize that the LS state of the Co^{4+} was assumed rather than demonstrated in most of the previous studies, which can be considered as a highly optimistic approach since Co^{4+} is a cation, which is susceptible to exhibit various spin states.¹

In this context, we reinvestigated the VSST in a $(\text{Pr}_{1-y}\text{Ln}_y)_{1-x}\text{Ca}_x\text{CoO}_3$ compound with the objective to identify in detail the nature of the spin states of not only the Co^{3+} but also of the Co^{4+} ions. We have carried out soft x-ray absorption (XAS) experiments at the Pr- $M_{4,5}$, Co- $L_{2,3}$, and O- L_s edges and made a detailed analysis using a combination of well-defined reference spectra and multiplet calculations. We made an effort to perform the experiments at many closely spaced temperature intervals, from well below to above T^* , in order to determine how much of the spin state transition is coupled to the Pr valence transition and how much it is driven by temperature as in LaCoO_3 . This study was carried out on $(\text{Pr}_{0.7}\text{Sm}_{0.3})_{0.7}\text{Ca}_{0.3}\text{CoO}_3$, a choice motivated by two main advantages as compared to $\text{Pr}_{0.5}\text{Ca}_{0.5}\text{CoO}_3$: first, an easier synthesis procedure;²² second, a larger content of Co^{3+} , which is favorable to investigate the controversial issue of its spin state above T^* . Note also that $(\text{Pr}_{0.7}\text{Sm}_{0.3})_{0.7}\text{Ca}_{0.3}\text{CoO}_3$

exhibits a VSST located at $T^* \sim 90$ K (like $\text{Pr}_{0.5}\text{Ca}_{0.5}\text{CoO}_3$ in most of the previous studies) and a lot of its physical properties are well documented in the literature.^{21,22}

II. EXPERIMENTAL DETAILS

Polycrystalline samples of $(\text{Pr}_{0.7}\text{Sm}_{0.3})_{0.7}\text{Ca}_{0.3}\text{CoO}_3$ (whose formula can also be written $\text{Pr}_{0.49}\text{Sm}_{0.21}\text{Ca}_{0.3}\text{CoO}_3$) were prepared by solid-state reaction using stoichiometric proportions of Pr_6O_{11} , Sm_2O_3 , CaO , and Co_3O_4 . The powders were intimately ground and the mixture was pelletized in form of $2 \times 2 \times 10$ mm bars. These bars were then sintered at 1200°C in flowing oxygen for 36 h. To ensure good oxygen stoichiometry, the samples were finally annealed in high pressure (130 bar) O_2 atmosphere for 48 h at 600°C . Powder x-ray diffraction patterns attested to the purity of the material, which shows a single phase with orthorhombic symmetry (space group $Pnma$) and parameters yielding a unit cell volume of $215.99(5) \text{ \AA}^3$ in accord with the literature.²¹

Electrical resistivity (ρ), magnetization (M), and heat capacity (C) measurements were carried out in a commercial physical properties measurements system (PPMS): the resistivity was measured by a standard four-probe method, the magnetization by an extraction method, and the heat capacity by a relaxation method supplemented by a “single-pulse” technique.³¹ These data were collected upon warming, in a magnetic field equal to zero for ρ and C , and equal to 1 T for M . The magnetic data can be presented in the form of dc susceptibility $\chi = M/H$, since the $M(H)$ curves were found to exhibit a perfect linear behavior over the temperature range of interest in the present study ($T > 20$ K).

The temperature-dependent XAS spectra at the Co- $L_{2,3}$, O- L_s , and Pr- $M_{4,5}$ edges were measured at the BL11A beamline of National Synchrotron Radiation Research Center (NSRRC) in Taiwan. The Co- $L_{2,3}$ and Pr- $M_{4,5}$ spectra were taken in the total electron yield (TEY) mode, while the O- K spectra were collected in the fluorescence yield (FY) mode, with a photon energy resolution of 0.3 and 0.15 eV, respectively. Spectra were recorded at eight temperatures between 10 and 290 K, with a 10 K spacing around the transition. The pellet samples were cleaved *in situ* in an ultrahigh-vacuum chamber with pressure in the 10^{-10} mbar range. NiO and CoO single crystals were measured *simultaneously* to serve as energy references for the O- K and Co- $L_{2,3}$ edges, respectively.

III. RESULTS AND DISCUSSION

Figure 1 shows a prominent transition close to 90 K on the $\chi(T)$, $\rho(T)$, and $C(T)$ curves. The value of this transition temperature, as well as the concomitant decrease in resistivity and increase in susceptibility that is observed upon warming, are in line with previous reports on this compound.^{21,22} In the present study, the sharpness of the transition is also supported by the heat capacity data, which exhibits a remarkably high peak centred at $T^* \sim 89.3$ K, with a full width at half maximum that does not exceed 1 K [see Fig. 1(d)].

A. Valence transition in Pr

Let us first address the change in the valence state of Pr when crossing T^* , by considering the evolution with temperature of

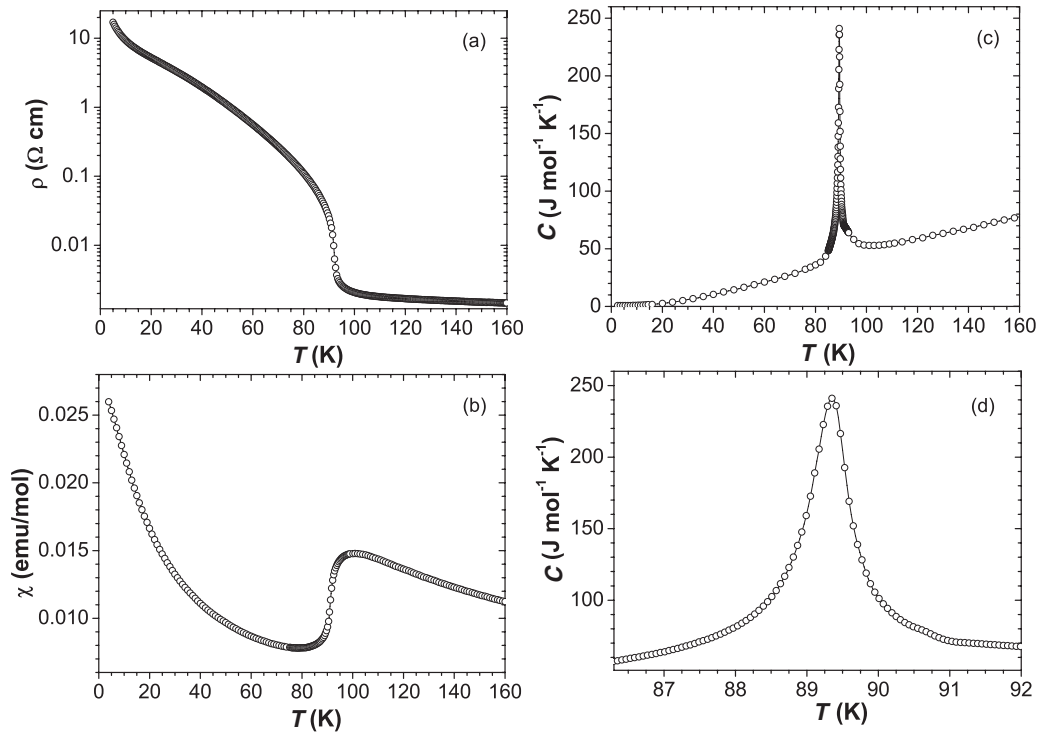


FIG. 1. (a) Temperature dependence of the resistivity in zero field. (b) Temperature dependence of the dc susceptibility (measured in 1 T). (c) Temperature dependence of the heat capacity in zero field. (d) Enlargement of (c) around the peak.

the Pr- $M_{4,5}$ XAS spectrum. In Fig. 2, one clearly observes the appearance of a broad shoulder at the high-energy side of the M_4 and M_5 peaks when cooling below T^* , a feature which can be attributed to an increase in the average valence of Pr, i.e., in our case, a partial transformation of Pr^{3+} towards Pr^{4+} . The enlargement of the M_5 high-energy foot displayed in the inset shows a very abrupt change as a function of temperature, the transition taking place between 80 and 90 K, consistently with the T^* value.³² In contrast, the temperature dependence

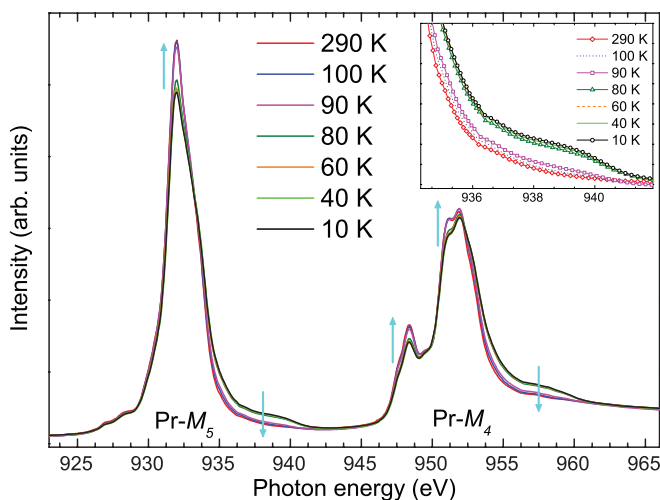


FIG. 2. (Color online) Temperature-dependent Pr- $M_{4,5}$ XAS spectrum. The arrows displayed close to the main features of the spectrum indicate the direction of increasing temperature. The inset is an enlargement of the high-energy foot of M_5 .

of the Pr spectra, both below and above T^* , is found to be very weak.

Let us now quantify the amount of tetravalent praseodymium below T^* by considering that the valence state of Pr in this regime is a mixture between Pr^{3+} and Pr^{4+} . Assuming that the spectrum at 290 K is representative of Pr^{3+} only, as done in the previous studies, the evaluation of the Pr^{4+} content at 10 K was derived as follows: first, the 290 K spectrum multiplied by a factor < 1 was subtracted from the 10 K spectrum till reaching a “difference spectrum” showing the typical features of pure Pr^{4+} , as observed in the measurements of PrO_2 (e.g., ratio close to 4 between the main peak and the high energy shoulder at M_5);^{33,34} then, the fraction of Pr^{4+} present at 10 K is associated to the spectral weight of this difference spectrum in the total one (at the same temperature of 10 K). Doing so, the estimated Pr^{4+} content was found to be 0.13 $\text{Pr}^{4+}/\text{f.u.}$

Our compound containing also samarium, which is another rare-earth susceptible to exhibit different valence states (e.g., Sm^{2+}), we investigated the Sm- $M_{4,5}$ edges between 1060 and 1130 eV as a function of temperature. We observed in all cases a spectrum well compatible with Sm^{3+} as reported in Sm_2O_3 ,³⁵ without any change in temperature, demonstrating that Sm does not take part in the VSST process.

B. Valence and spin state transitions in Co

To probe the valence and spin states of the Co ions, we considered the Co- $L_{2,3}$ and O- K absorption edges. It can be noted that the Co ($2p \rightarrow 3d$) transitions at the Co- $L_{2,3}$ edge involve directly the relevant valence shell and are extremely sensitive to the charge and spin states.^{11,36–40}

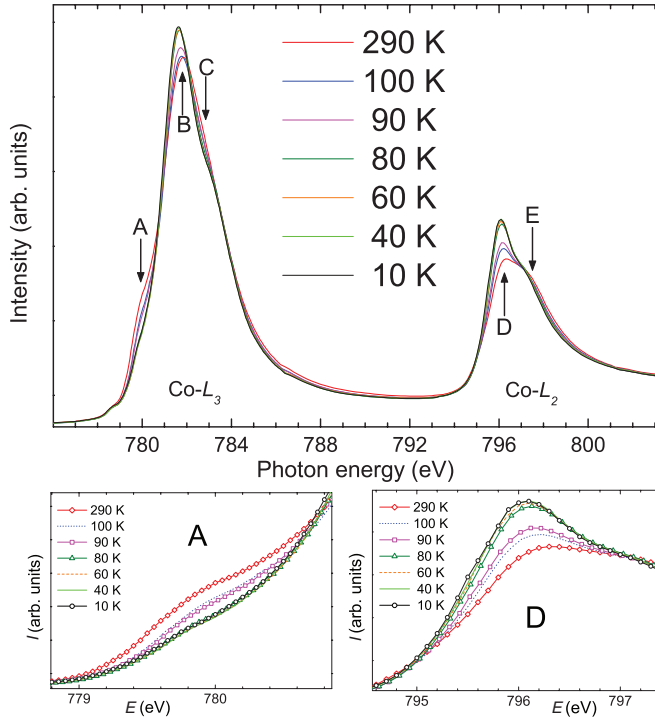


FIG. 3. (Color online) Temperature-dependent Co- $L_{2,3}$ XAS spectrum. Labels A, B, C, D, and E mark features discussed in the text. In each case, the direction of the arrow corresponds to decreasing temperature. (Bottom) Enlargements of the energy ranges corresponding to the A and D features.

Figure 3 shows the evolution of the XAS spectrum as a function of temperature, between 10 and 290 K. One observes that these spectra closely resemble those collected in LaCoO_3 ,^{6,11} the most significant difference being a relative larger intensity of the shoulders located just above the main peaks at L_3 and L_2 (noted C and E), which can be attributed to the presence of Co^{4+} in $(\text{Pr}_{0.7}\text{Sm}_{0.3})_{0.7}\text{Ca}_{0.3}\text{CoO}_3$. There is also a striking similarity in the temperature dependence of this spectrum, which manifests itself by two main features: (i) at low temperatures, the XAS spectra taken below 80 K in $(\text{Pr}_{0.7}\text{Sm}_{0.3})_{0.7}\text{Ca}_{0.3}\text{CoO}_3$ clearly look like that of LaCoO_3 at 20 K,¹¹ showing a narrow peak at ~ 796 eV at the L_2 edge (noted D), which is a feature known to be the hallmark of Co^{3+} LS; and (ii) at high temperatures, the XAS spectra above 90 K in $(\text{Pr}_{0.7}\text{Sm}_{0.3})_{0.7}\text{Ca}_{0.3}\text{CoO}_3$ exhibit a low energy shoulder at ~ 780 eV (noted A) below the main peak of the Co- L_3 edge (noted B), which is identical to what is observed in LaCoO_3 above ~ 600 K.^{6,11} This feature is typical of the presence of Co^{3+} in a spin state higher than LS, and is expected to be more pronounced for HS than for IS.^{11,36}

This similarity between LaCoO_3 and $(\text{Pr}_{0.7}\text{Sm}_{0.3})_{0.7}\text{Ca}_{0.3}\text{CoO}_3$ in the temperature dependence of the Co- $L_{2,3}$ spectrum indicates that a change in Co^{3+} from a LS state to a higher spin state does take place in the latter compound upon arising temperature. There is, however, a notable difference in the *shape* of this temperature dependence, since $(\text{Pr}_{0.7}\text{Sm}_{0.3})_{0.7}\text{Ca}_{0.3}\text{CoO}_3$ exhibits a rapid change around T^* , contrary to LaCoO_3 in which one observes only a smooth transition spread out over a wide temperature range. Looking

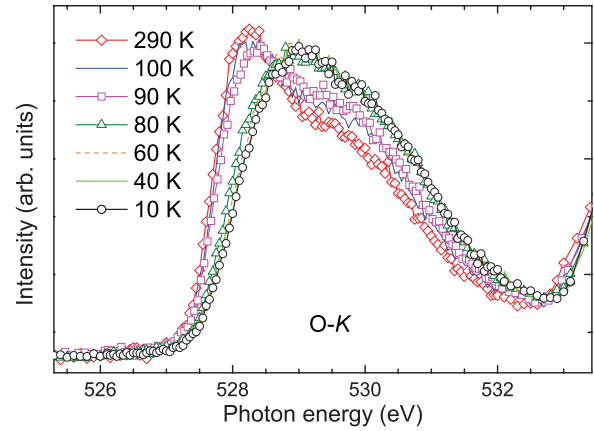


FIG. 4. (Color online) Temperature dependence of the pre-edge region of the O- K XAS spectrum.

in more detail at the data of $(\text{Pr}_{0.7}\text{Sm}_{0.3})_{0.7}\text{Ca}_{0.3}\text{CoO}_3$ (bottom panels of Fig. 3), one observes that the spectral change is very small from 10 to 80 K, before exhibiting an abrupt variation between 80 to 90 K, and finally, a weaker—but well visible—temperature dependence up to 290 K.

Figure 4 displays the temperature-dependent O- K spectrum, which is also sensitive to a spin state transition in Co^{3+} .^{6,15,36} Here, we are mainly interested in the lowest lying states, i.e., the pre-edge region lying below 532 eV, which corresponds to transitions from the O $1s$ core level to the O $2p$ orbitals mixed with unoccupied Co $3d$ states.^{6,36,39,40} As the temperature is increased, one observes a sudden transfer of spectral weight from the higher energy peak at ~ 529.1 eV to the lower energy peak at ~ 528.2 eV. Such a temperature-induced transfer—also present in LaCoO_3 (between 420 and 550 K)⁶ and $\text{Ba}_2\text{Co}_9\text{O}_{14}$ ⁴¹—is an additional support to the presence of a spin state transition involving Co^{3+} in $(\text{Pr}_{0.7}\text{Sm}_{0.3})_{0.7}\text{Ca}_{0.3}\text{CoO}_3$. Indeed, the electron promotion from t_{2g} and e_g orbitals that characterizes such an SST is expected to yield this type of spectral weight transfer. A striking feature of Fig. 4 is the steepness of the spectral weight transfer that is found to be much sharper than in LaCoO_3 .⁶ It can also be noted that the spectral change observed between 80 to 90 K in $(\text{Pr}_{0.7}\text{Sm}_{0.3})_{0.7}\text{Ca}_{0.3}\text{CoO}_3$ is even more pronounced at the O $1s$ edge (see Fig. 4) than at the Co- $L_{2,3}$ edge (see Fig. 3). This can be ascribed to the fact that the spectral weight below 532 eV at the O- K edge is expected to be affected not only by the spin state transition of Co^{3+} ⁶ but also by the valence change in Pr; indeed Pr^{4+} has a clear signature in this energy range due to a strong $4f/O-2p$ covalence, whereas Pr^{3+} has not.⁴²

After having established the existence of an SST in the Co ions, the problem is now to determine the nature of the spin states of Co^{3+} and Co^{4+} that are involved in this transition. We note that the only issue on which there is a general consensus so far is that Co^{3+} is in a pure LS state at $T \ll T^*$. Before addressing the delicate issue of the Co^{3+} spin state above T^* , let us start with the case of Co^{4+} , which is another important, but often overlooked issue.

1. Spin state of Co^{4+}

In most of the previous studies on VSST in cobaltites, it was assumed that the Co^{4+} are in an LS state, and that they stay in

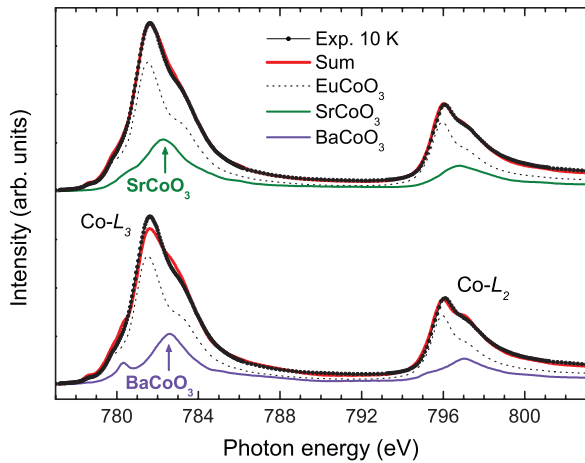


FIG. 5. (Color online) Experimental Co- $L_{2,3}$ XAS spectrum at 10 K compared to simulations using *experimental reference spectra* for Co^{3+} (EuCoO_3) (from Ref. 37) combined with either Co^{4+} IS (SrCoO_3) (from Ref. 1) or Co^{4+} LS (BaCoO_3) (from Ref. 38).

this state over the whole T range investigated so far, i.e., 300 K. However, we previously noted that the possibility of higher spin state should be considered for Co^{4+} , in particular, the intermediate spin state. Even though the archetypical example of Co^{4+} IS remains the perovskite SrCoO_3 ,¹ the occurrence of this state was recently reported in other oxides such as Sr_2CoO_4 ⁴³ and $\text{Ca}_3\text{Co}_4\text{O}_9$.⁴⁴ On the other hand, it is widely admitted that Co^{4+} is LS in BaCoO_3 .⁴⁵ From a structural viewpoint, we emphasize that $(\text{Pr}_{0.7}\text{Sm}_{0.3})_{0.7}\text{Ca}_{0.3}\text{CoO}_3$ is much closer to SrCoO_3 (cubic perovskite with corner-shared CoO_6 octahedra) than to BaCoO_3 (hexagonal 2H-structure showing chains of face-sharing CoO_6), which is a first indication pointing to the possibility of a IS state in our material.

To investigate this issue more precisely, one can compare Co- $L_{2,3}$ spectra at 10 K to those calculated considering experimental reference spectra for Co^{3+} LS (EuCoO_3),³⁷ Co^{4+} LS (BaCoO_3)³⁸ and Co^{4+} IS (SrCoO_3).¹ In this analysis, we considered the ratio $\text{Co}^{4+}/\text{Co}^{3+}$ as a free parameter. Figure 5 shows the best fitting obtained with each of these two spin states of Co^{4+} , and it is clear that one obtains better agreement with Co^{4+} IS. Moreover, the content of Co^{4+} derived from this fitting is found to be 0.16 per f.u., i.e., well consistent with the value 0.17 ($=0.30-0.13$) that is expected from the previously estimated amount of Pr^{4+} (0.13/f.u.). Therefore it appears that IS is the most likely spin state of Co^{4+} below T^* . In addition, since the Co^{4+} HS state is supposed to lie at much higher energy²⁰—not reachable till room temperature—we will consider that the Co^{4+} ion remains in this IS state over the whole temperature range of the present study.

2. Spin state of Co^{3+}

For Co^{3+} , one has to face the problem of the absence of undisputed reference compounds for the IS and HS spin-states in an octahedral environment. This prevents us from directly comparing the data to composite spectra made of experimental reference spectra, as done above for Co^{4+} . Therefore, to address the nature of the Co^{3+} spin state, one has to shift to another strategy where the experimental temperature

dependent Co- $L_{2,3}$ XAS spectra are compared to theoretical simulations. In the present study, such calculated curves were derived from a configuration-interaction (CI) cluster model, including full-atomic multiplet theory, crystal-field effect and hybridization with the O $2p$ ligands.^{46–48} The validity of this approach is supported by its proven ability to reproduce the experimental XAS spectra of reference compounds, i.e., those containing cations for which there is no doubt about the valence and spin states. Limiting ourselves to the case of $\text{Co}^{3+}/\text{Co}^{4+}$, such compounds are BaCoO_3 (for Co^{4+} LS),³⁸ SrCoO_3 (for Co^{4+} IS),¹ EuCoO_3 (for Co^{3+} LS),³⁶ as well as $\text{Sr}_2\text{CoO}_3\text{Cl}$ (for Co^{3+} HS in a pyramidal environment).³⁶ Using theoretical spectra calculated by the CI cluster model was also found to be a fruitful approach to address the nature of the Co spin states in various compounds where this issue was under question, like for instance in $\text{La}_{1.5}\text{Sr}_{0.5}\text{CoO}_4$ and Na_xCoO_2 .^{38,39} The main parameters of the CI cluster model are the O $2p$ to Co $3d$ charge-transfer energy (Δ), the $3d-3d$ and $3d-2p$ Coulomb energies (U_{dd} and U_{cd} , respectively), the ionic part of the crystal-field ($10Dq$), and the O $2p$ to Co $3d$ transfer integral involving the e_g orbitals ($pd\sigma$). It must be emphasized that the actual crystal-field splitting is significantly larger than $10Dq$ owing to the ligand field contribution (covalency effects) associated to the hybridization with the O $2p$ orbitals.

The values of parameters used to calculate the theoretical spectra of Co^{4+} IS, Co^{3+} HS and Co^{3+} LS in the present study are given in Ref. 49. They are similar to those previously reported in the literature,^{1,11,36,37} and are also well consistent with general trends expected when varying the valence or spin-state of a $3d$ cation. As a matter of fact, the main expected change between the LS and HS states of Co^{3+} is a smaller crystal-field splitting, which is presently accounted for by a decrease in both $10Dq$ and $|pd\sigma|$, the latter effect being actually predominant.^{6,11} About the influence of the valence state, the main effect when going from +3 to +4 for late transition metals is a marked decrease in Δ , which can yield negative values in the case of Co.^{47,48} Our values are also consistent with the relationship $\Delta^{n+} \approx \Delta^{(n-1)+} - U_{dd}$, previously reported for the couples $\text{Fe}^{3+}/\text{Fe}^{2+}$ and $\text{Co}^{4+}/\text{Co}^{3+}$.^{38,50}

To quantify hereafter the percentages of Co^{3+} (LS and HS) and Co^{4+} (IS) in the case of $(\text{Pr}_{0.7}\text{Sm}_{0.3})_{0.7}\text{Ca}_{0.3}\text{CoO}_3$, the contribution of 2% of Co^{2+} (using experimental spectra from CoO) was first subtracted from the experimental Co- $L_{2,3}$ XAS spectra shown in Fig. 6. Note that the presence of such a level of Co^{2+} impurity is often observed in cobaltites and is, generally, ascribed to a slight under stoichiometry of oxygen.

The calculation procedure was first tested with the spectrum at 10 K, for which the population of all the present Co species can be anticipated, as discussed in Sec. B.1. As displayed in Fig. 6(a), it turns out that the calculated spectrum obtained by combining the sum of 83% Co^{3+} LS and 17% Co^{4+} IS with an edge jump curve is in perfect agreement with the experimental data. We emphasize that the matching to the data is as good as that obtained when combining experimental spectra of reference compounds (top panel of Fig. 5), a feature which confirms the reliability of the simulated spectra derived from the CI cluster model.

When the temperature is increased above T^* , let us first consider that the spin state transition of Co^{3+} leads to a

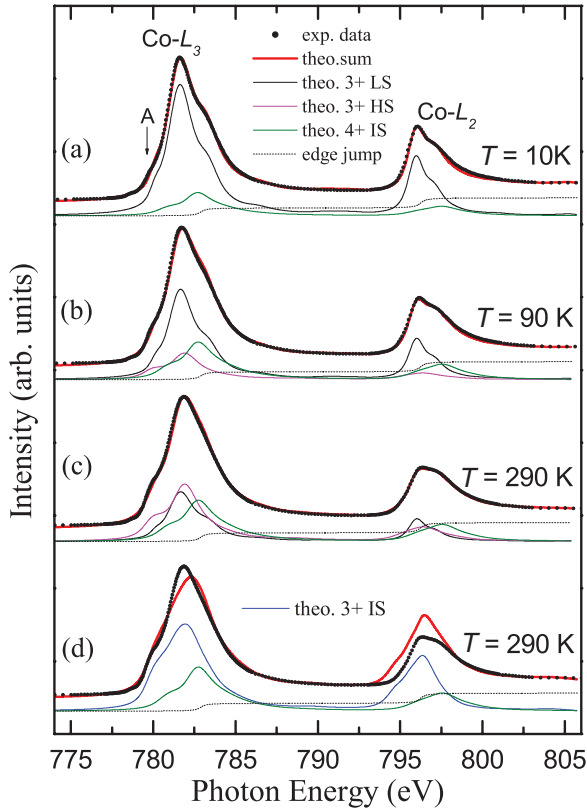


FIG. 6. (Color online) Experimental (black circles) Co- $L_{2,3}$ XAS spectra compared to simulations (red lines) at various temperatures: (a) 10, (b) 90, (c) and (d) 290 K. The simulations combine theoretical spectra for Co^{3+} LS (black), Co^{3+} HS (magenta), Co^{4+} IS (green) as well as Co^{3+} IS (blue) in (d). The dashed lines represent edge jump in all cases. The label A in (a) marks the same feature as in Fig. 3.

mixture between LS and HS spin states. As previously done in LaCoO_3 , the temperature dependence of the Co- $L_{2,3}$ spectrum was analyzed by using an incoherent sum of the LS and HS contributions for Co^{3+} .¹¹ This was combined with a contribution from Co^{4+} IS, whose content was found to increase abruptly (by $\sim 10\%$) when crossing T^* . Doing so, we were able to obtain good simulations of the spectra at all temperatures, as exemplified in Figs. 6(b) and 6(c) for 90 and 290 K, respectively.

Although the results of Fig. 6 are well consistent with the achievement of a mixed LS/HS state for Co^{3+} above T^* , let us consider the alternative possibility of a Co^{3+} IS state. To do so, we considered the spectrum at room temperature. We first calculated the Co^{3+} IS spectrum (blue line) that is displayed in Fig. 6(d). Note that, in the cubic symmetry, the Co^{3+} IS states lie too high in energy and cannot be stabilized; therefore, the Co^{3+} IS spectrum is not taken from the ground states, but rather from high-lying excited states. In order to stabilize the Co^{3+} IS ground state, one has to introduce a huge e_g splitting (more than 2 eV), via a Jahn-Teller distortion, in the full multiplet calculation. Then, we compared the experimental spectrum taken at 290 K with the sum of theoretical spectra for Co^{3+} IS and Co^{4+} IS, keeping the ratio between them as an adjustable parameter. It turns out that even the best simulation shown in Fig. 6(d) exhibits a poor overlapping with the experimental data, in marked contrast with the almost perfect

superimposition shown by the LS/HS scenario in Fig. 6(c). Accordingly, one can consider that these results provide us with a direct evidence against the occurrence of a (LS \rightarrow IS) transition in the VSST of $(\text{Pr}_{1-y}\text{Ln}_y)_{1-x}\text{Ca}_x\text{CoO}_3$ compounds.

In the literature, the onset of metallic-like conductivity above T^* is often used as an argument to support the (LS \rightarrow IS) scenario, since easy electronic delocalization is expected between Co^{3+} IS and Co^{4+} LS. It must be emphasized, however, that our picture characterized by Co^{3+} HS and Co^{4+} IS yields a very similar situation from the viewpoint of electronic mobility.⁵¹ In both cases indeed, one is dealing with two cations having the same core spin at the t_{2g} triplet and that just differ by one electron on the e_g doublet, a situation allowing to interchange the states by moving only one e_g electron. Accordingly, we note that the couple (Co^{3+} HS/ Co^{4+} IS) considered in the present work is as compatible as (Co^{3+} IS/ Co^{4+} LS) with the good electronic conductivity that is observed above T^* .

C. Temperature dependence of the transition

Simulations of the Co- $L_{2,3}$ XAS spectra were carried out for all of the experimental spectra at the temperatures measured, using combinations of contributions from the Co^{4+} IS, Co^{3+} LS, and Co^{3+} HS. In Fig. 7(a), we reported the percentages of each of these species that lead to the best agreement with the data. In Fig. 7(b), we also plot the temperature variation of the Pr^{3+} content derived from the Pr- $M_{4,5}$ spectra using the procedure described in Sec. III A. One observes a steep increase in Pr^{3+} at T^* , with a much weaker temperature dependence both below and above the transition. This overall variation turns out to be very close to that previously derived in $\text{Pr}_{0.5}\text{Ca}_{0.5}\text{CoO}_3$ ^{28,29} and $(\text{Pr}_{1-y}\text{Y}_y)_{0.7}\text{Ca}_{0.3}\text{CoO}_3$ ($y = 0.075$ and 0.15)⁵² using different methods of analysis of XAS data.

In Fig. 7(a), we can observe that the Co^{3+} LS content is reduced from 83% to 55% between 10 K to 90 K, and is further reduced to 32% at 290 K, while the Co^{3+} HS content is increased from 0% to 16% and then to 37%. The Co^{4+} fraction increases from 17% to 29% between 10 and 90 K, and then remains essentially constant up to 290 K. Consistently with the charge balance, the variation of Pr^{3+} in Fig. 7(b) exhibits a profile similar to that of Co^{4+} . Quantitatively speaking, the Pr^{3+} content per f.u. increases from 0.36 to 0.44 between 10 K and 90 K, and reaches 0.47 at 100 K, i.e., a value closely approaching that of a pure trivalent state (0.49 per f.u.).

Figure 7 shows that the temperature dependencies of the Co^{3+} LS, Co^{3+} HS, and Co^{4+} IS fractions between 10 and 90 K are all very similar to that of the $\text{Pr}^{4+}/\text{Pr}^{3+}$ valence change, at least within the accuracy of the experiment and analysis. Following a low-temperature regime showing a smooth evolution (which must be regarded cautiously since these variations are actually within the experimental uncertainty), the main feature found in all cases is a large change centered at T^* , i.e., between 80 and 90 K.

The overall behavior displayed in Fig. 7 thus indicates that the spin state transition of Co^{3+} in the 10 to 90 K temperature range is intimately coupled to the $\text{Pr}^{4+}/\text{Pr}^{3+}$ valence change. A different behavior sets in at higher temperatures, i.e., at $T > T^*$, where one can observe that the temperature dependence of the Co^{3+} HS and LS contents is significantly

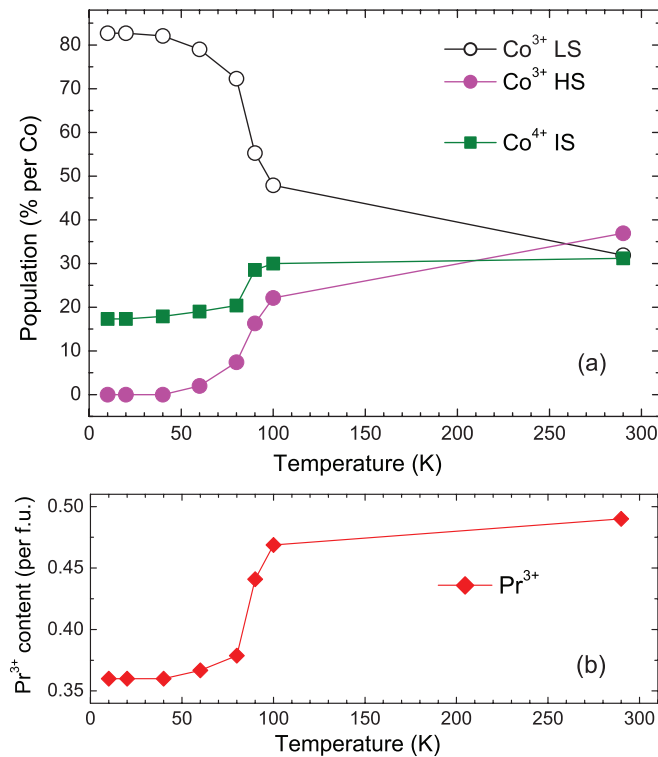


FIG. 7. (Color online) (a) Temperature dependence of the populations of Co³⁺ LS, Co³⁺ HS and Co⁴⁺ IS derived from the simulations of the experimental Co- $L_{2,3}$ XAS spectra, and (b) temperature dependence of the Pr³⁺ content extracted from the Pr- $M_{4,5}$ XAS spectra.

more pronounced than that of Pr³⁺ and Co⁴⁺, the latter species being actually already close to their saturation values. Considering the variations between 100 and 290 K, the Pr³⁺ and Co⁴⁺ contents only change by less than 5%, whereas the population of Co³⁺ HS is increased by more than 66%.

In the high-temperature regime ($T > T^*$), it deserves to be noted that (Pr_{0.7}Sm_{0.3})_{0.7}Ca_{0.3}CoO₃ exhibits properties similar to those of Sr-doped LaCoO₃;⁵³ a substantial fraction of the Co³⁺ is in the HS state, the spin state transition is gradual, and the resistivity is no longer that of a semiconductor but rather that of a bad metal. The low-temperature behavior of (Pr_{0.7}Sm_{0.3})_{0.7}Ca_{0.3}CoO₃ is, however, very different from that of Sr-doped LaCoO₃ or even from that of undoped LaCoO₃. Despite the high percentage of Co⁴⁺ (~17%), all of the

Co³⁺ remains in the LS state. Increasing the temperature to 40 K or even 60 K, the amount of Co³⁺ HS remains minute (<2%), much smaller than in LaCoO₃. In this respect, (Pr_{0.7}Sm_{0.3})_{0.7}Ca_{0.3}CoO₃ is more similar to EuCoO₃, which has a very stable Co³⁺ LS configuration over a wide range of temperatures. Apparently, the mechanism responsible for the formation of Pr⁴⁺ at low temperatures somehow also prevents the Co⁴⁺ ions to interact with the Co³⁺ thereby leaving the Co³⁺ in a stable LS configuration.

IV. CONCLUSION

We investigated the valence and spin state transition (VSST) in (Pr_{0.7}Sm_{0.3})_{0.7}Ca_{0.3}CoO₃, whose most salient manifestation is a sharp first-order transition at $T^* \sim 89.3$ K, visible in all physical properties. Using XAS measurements at the Co- $L_{2,3}$, Pr- $M_{4,5}$, and O- K edges, we found evidence for valence state transitions in Co and Pr in the vicinity of T^* . The spin state transition in Co³⁺ follows this valence transition from low temperature up to T^* . Above T^* , we essentially observe a gradual continuation of the spin state transition of the Co³⁺. At low temperatures, we observed that Co³⁺ and Co⁴⁺ are in LS and IS states, respectively, while Pr has a mixed valence state Pr³⁺/Pr⁴⁺ with about 0.13 Pr⁴⁺/fu. Crossing T^* upon warming, the transition exhibits a jump, associated with the stabilization of ions having larger ionic radius, i.e., Co³⁺ HS and Pr³⁺ at the expense of Co³⁺ LS and Pr⁴⁺, a behavior that is consistent with the sudden volume expansion previously observed in related compounds.^{17,25,28} Our analysis of the XAS spectra indicates that the spin-state transition of the Co³⁺ involves the LS and HS states, and that the IS state does not play a role. Contrary to the literature, we found that the spin state of Co⁴⁺ is IS instead of LS. The presence of the IS for the Co⁴⁺ together with the HS for the Co³⁺ leaves open the possibility for a good electronic conduction as is observed at elevated temperatures. Obviously, the issue of the formation of Pr⁴⁺ and the role of the bonding with the oxygens⁵⁴ will deserve further investigation both from theoretical and experimental viewpoints as this seems to be a key ingredient of the VSST.

ACKNOWLEDGMENTS

This work was supported by the European program ‘‘SO-PRANO’’ under Marie Curie actions (Grant. No. PITN-GA-2008-214040).

¹R. H. Potze, G. A. Sawatzky, and M. Abbate, *Phys. Rev. B* **51**, 11501 (1995).

²M. A. Korotin, S. Yu. Ezhov, I. V. Solovyev, V. I. Anisimov, D. I. Khomskii, and G. A. Sawatzky, *Phys. Rev. B* **54**, 5309 (1996).

³K. Knížek, P. Novák, and Z. Jiráček, *Phys. Rev. B* **71**, 054420 (2005).

⁴J. B. Goodenough, *J. Phys. Chem. Solids* **6**, 287 (1958).

⁵R.R. Heikes, R. C. Miller, and R. Mazelsky, *Physica (Amsterdam)* **30**, 1600 (1964); P. M. Raccach and J. B. Goodenough, *Phys. Rev.* **155**, 932 (1967); V. G. Bhide, D. S. Rajoria, G. R. Rao, and C. N. R. Rao, *Phys. Rev. B* **6**, 1021 (1972).

⁶M. Abbate, J. C. Fuggle, A. Fujimori, L. H. Tjeng, C. T. Chen, R. Potze, G. A. Sawatzky, H. Eisaki, and S. Uchida, *Phys. Rev. B* **47**, 16124 (1993).

⁷M. A. Seánaris-Rodríguez and J. B. Goodenough, *J. Solid State Chem.* **116**, 224 (1995).

⁸K. Asai, A. Yoneda, O. Yokokura, J. M. Tranquada, G. Shirane, and K. Kohn, *J. Phys. Soc. Jpn* **67**, 290 (1998).

⁹P. G. Radaelli and S.-W. Cheong, *Phys. Rev. B* **66**, 094408 (2002).

¹⁰T. Kyomen, Y. Asaka, and M. Itoh, *Phys. Rev. B* **71**, 024418 (2005).

- ¹¹M. W. Haverkort, Z. Hu, J. C. Cezar, T. Burnus, H. Hartmann, M. Reuther, C. Zobel, T. Lorenz, A. Tanaka, N. B. Brookes, H. H. Hsieh, H.-J. Lin, C. T. Chen, and L. H. Tjeng, *Phys. Rev. Lett.* **97**, 176405 (2006).
- ¹²M. Medarde, C. Dallera, M. Grioni, J. Voigt, A. Podlesnyak, E. Pomjakushina, K. Conder, Th. Neisius, O. Tjernberg, and S. N. Barilo, *Phys. Rev. B* **73**, 054424 (2006).
- ¹³Z. Jiráček, J. Hejtmánek, K. Knížek, and M. Veverka, *Phys. Rev. B* **78**, 014432 (2008).
- ¹⁴T. Saitoh, T. Mizokawa, A. Fujimori, M. Abbate, Y. Takeda, and M. Takano, *Phys. Rev. B* **55**, 4257 (1997); S. Yamaguchi, Y. Okimoto, and Y. Tokura, *ibid.* **55**, R8666 (1997); Y. Kobayashi, N. Fujiwara, S. Murata, K. Asai, and H. Yasuoka, *ibid.* **62**, 410 (2000); C. Zobel, M. Kriener, D. Bruns, J. Baier, M. Grüninger, T. Lorenz, P. Reutler, and A. Revcolevschi, *ibid.* **66**, 020402(R) (2002); J. Baier, S. Jodlauk, M. Kriener, A. Reichl, C. Zobel, H. Kierspel, A. Freimuth, and T. Lorenz, *ibid.* **71**, 014443 (2005); G. Vankó, J.-P. Rueff, A. Mattila, Z. Németh, and A. Shukla, *ibid.* **73**, 024424 (2006).
- ¹⁵R. F. Klie, J. C. Zheng, Y. Zhu, M. Varela, J. Wu, and C. Leighton, *Phys. Rev. Lett.* **99**, 047203 (2007).
- ¹⁶S. Noguchi, S. Kawamata, K. Okuda, H. Nojiri, and M. Motokawa, *Phys. Rev. B* **66**, 094404 (2002); A. Podlesnyak, S. Streule, J. Mesot, M. Medarde, E. Pomjakushina, K. Conder, A. Tanaka, M. W. Haverkort, and D. I. Khomskii, *Phys. Rev. Lett.* **97**, 247208 (2006).
- ¹⁷S. Tsubouchi, T. Kyomen, M. Itoh, P. Ganguly, M. Oguni, Y. Shimojo, Y. Morii, and Y. Ishii, *Phys. Rev. B* **66**, 052418 (2002).
- ¹⁸H. Masuda, T. Fujita, T. Miyashita, M. Soda, Y. Yasui, Y. Kobayashi, and M. Sato, *J. Phys. Soc. Jpn* **72**, 873 (2003).
- ¹⁹S. Tsubouchi, T. Kyomen, M. Itoh, and M. Oguni, *Phys. Rev. B* **69**, 144406 (2004).
- ²⁰T. Fujita, T. Miyashita, Y. Yasui, Y. Kobayashi, M. Sato, E. Nishibori, M. Sakata, Y. Shimojo, N. Igawa, Y. Ishii, K. Kakurai, T. Adachi, Y. Ohishi, and M. Takata, *J. Phys. Soc. Jpn* **73**, 1987 (2004).
- ²¹T. Fujita, S. Kawabata, M. Sato, N. Kurita, M. Hedo, and Y. Uwatoko, *J. Phys. Soc. Jpn* **74**, 2294 (2005).
- ²²G. Y. Wang, T. Wu, X. G. Luo, W. Wang, and X. H. Chen, *Phys. Rev. B* **73**, 052404 (2006); G. Y. Wang, X. H. Chen, T. Wu, G. Wu, X. G. Luo, and C. H. Wang, *ibid.* **74**, 165113 (2006).
- ²³T. Naito, H. Sasaki, and H. Fujishiro, *J. Phys. Soc. Jpn* **79**, 034710 (2010).
- ²⁴A. V. Kalinov, O. Yu. Gorbenko, A. N. Taldenkov, J. Rohrkamp, O. Heyer, S. Jodlauk, N. A. Babushkina, L. M. Fisher, A. R. Kaul, A. A. Kamenev, T. G. Kuzmova, D. I. Khomskii, K. I. Kugel, and T. Lorenz, *Phys. Rev. B* **81**, 134427 (2010).
- ²⁵A. J. Barón-González, C. Frontera, J. L. García-Muñoz, J. Blasco, and C. Ritter, *Phys. Rev. B* **81**, 054427 (2010).
- ²⁶K. Knížek, J. Hejtmánek, P. Novák, and Z. Jiráček, *Phys. Rev. B* **81**, 155113 (2010).
- ²⁷J. Hejtmánek, E. Šantavá, K. Knížek, M. Maryško, Z. Jiráček, T. Naito, H. Sasaki, H. Fujishiro, *Phys. Rev. B* **82**, 165107 (2010).
- ²⁸J. L. García-Muñoz, C. Frontera, A. J. Barón-González, S. Valencia, J. Blasco, R. Feyerherm, E. Dudzik, R. Abrudan, and F. Radu, *Phys. Rev. B* **84**, 045104 (2011).
- ²⁹J. Herrero-Martín, J. L. García-Muñoz, S. Valencia, C. Frontera, J. Blasco, A. J. Barón-González, G. Subías, R. Abrudan, F. Radu, E. Dudzik, and R. Feyerherm, *Phys. Rev. B* **84**, 115131 (2011).
- ³⁰J. Herrero-Martín, J. L. García-Muñoz, K. Kvashnina, E. Gallo, G. Subías, J. A. Alonso, and A. J. Barón-González, *Phys. Rev. B* **86**, 125106 (2012).
- ³¹V. Hardy, Y. Bréard, and C. Martin, *J. Phys.: Condens. Matter* **21**, 075403 (2009).
- ³²It must be kept in mind, however, that there could be a slight shift between the nominal and actual values of temperature in XAS data, owing to uncertainty associated to the control of temperature in spectroscopy experiments. This could explain why the transition appears to be perfectly completed on the XAS spectrum at 90 K, while this temperature is still within the transition regime visible on the physical properties of Fig. 1.
- ³³R. C. Karnatak, J.-M. Esteve, H. Dexpert, M. Gasgnier, P. E. Caro, and L. Albert, *Phys. Rev. B* **36**, 1745 (1987).
- ³⁴Z. Hu, G. Kaindl, H. Ogasawara, A. Kotani, and I. Felner, *Chem. Phys. Lett.* **325**, 241 (2000).
- ³⁵M. Alexander, H. Romberg, N. Nücker, P. Adelman, J. Fink, J. T. Markert, M. B. Maple, S. Uchida, H. Takagi, Y. Tokura, A. C. W. P. James, and D. W. Murphy, *Phys. Rev. B* **43**, 333 (1991).
- ³⁶Z. Hu, H. Wu, M. W. Haverkort, H. H. Hsieh, H.-J. Lin, T. Lorenz, J. Baier, A. Reichl, I. Bonn, C. Felser, A. Tanaka, C. T. Chen, and L. H. Tjeng, *Phys. Rev. Lett.* **92**, 207402 (2004).
- ³⁷T. Burnus, Z. Hu, M. W. Haverkort, J. C. Cezar, D. Flahaut, V. Hardy, A. Maignan, N. B. Brookes, A. Tanaka, H. H. Hsieh, H.-J. Lin, C. T. Chen, and L. H. Tjeng, *Phys. Rev. B* **74**, 245111 (2006).
- ³⁸H.-J. Lin, Y. Y. Chin, Z. Hu, G. J. Shu, F. C. Chou, H. Ohta, K. Yoshimura, S. Hébert, A. Maignan, A. Tanaka, L. H. Tjeng, and C. T. Chen, *Phys. Rev. B* **81**, 115138 (2010).
- ³⁹C. F. Chang, Z. Hu, Hua Wu, T. Burnus, N. Hollmann, M. Benomar, T. Lorenz, A. Tanaka, H.-J. Lin, H. H. Hsieh, C. T. Chen, and L. H. Tjeng, *Phys. Rev. Lett.* **102**, 116401 (2009).
- ⁴⁰H. Ohta, K. Yoshimura, Z. Hu, Y. Y. Chin, H.-J. Lin, H. H. Hsieh, C. T. Chen, and L. H. Tjeng, *Phys. Rev. Lett.* **107**, 066404 (2011).
- ⁴¹J.-G. Cheng, J.-S. Zhou, Z. Hu, M. R. Suchomel, Y. Y. Chin, C. Y. Kuo, H.-J. Lin, J. M. Chen, D. W. Pi, C. T. Chen, T. Takami, L. H. Tjeng, and J. B. Goodenough, *Phys. Rev. B* **85**, 094424 (2012).
- ⁴²Z. Hu, R. Meier, C. Schüßler-Langeheine, E. Weschke, G. Kaindl, I. Felner, M. Merz, N. Nücker, S. Schuppler, and A. Erb, *Phys. Rev. B* **60**, 1460 (1999).
- ⁴³J. Matsuno, Y. Okimoto, Z. Fang, X. Z. Yu, Y. Matsui, N. Nagaosa, M. Kawasaki, and Y. Tokura, *Phys. Rev. Lett.* **93**, 167202 (2004); X. L. Wang and E. Takayama-Muromachi, *Phys. Rev. B* **72**, 064401 (2005).
- ⁴⁴R. F. Klie, Q. Qiao, T. Paulauskas, A. Gulec, A. Rebola, S. Ögüt, M. P. Prange, J. C. Idrobo, S. T. Pantelides, S. Kolesnik, B. Dabrowski, M. Ozdemir, C. Boyraz, D. Mazumdar, and A. Gupta, *Phys. Rev. Lett.* **108**, 196601 (2012).
- ⁴⁵C. Felser, K. Yamaura, and R. J. Cava, *J. Solid State Chem.* **146**, 411 (1999).
- ⁴⁶J. Zaanen, C. Westra, and G. A. Sawatzky, *Phys. Rev. B* **33**, 8060 (1986); F. M. F. de Groot, J. C. Fuggle, B. T. Thole, and G. A. Sawatzky, *ibid.* **42**, 5459 (1990); M. Abbate, R. Potze, G. A. Sawatzky, and A. Fujimori, *ibid.* **49**, 7210 (1994); A. Tanaka and T. Jo, *J. Phys. Soc. Jpn.* **63**, 2788 (1994).
- ⁴⁷A. E. Bocquet, T. Mizokawa, T. Saitoh, H. Namatame, and A. Fujimori, *Phys. Rev. B* **46**, 3771 (1992).
- ⁴⁸T. Saitoh, A. E. Bocquet, T. Mizokawa, and A. Fujimori, *Phys. Rev. B* **52**, 7934 (1995).

⁴⁹The Slater integrals were reduced to 75% of their Hartree Fock values. Parameters in eV: $U_{dd} = 5.5$ and $U_{cd} = 7$; $\Delta = 2$ (for Co^{3+}) and $\Delta = -4$ (for Co^{4+}); $10Dq = 0.5$ (for Co^{3+} LS), $10Dq = 0.4$ (for Co^{3+} HS), and $10Dq = 0.5$ (for Co^{4+} IS); $pd\sigma = -1.7$ (for Co^{3+} LS), $pd\sigma = -1.55$ (for Co^{3+} HS), and $pd\sigma = -1.23$ (for Co^{4+} IS).

⁵⁰J. Chen, D. J. Huang, A. Tanaka, C. F. Chang, S. C. Chung, W. B. Wu, and C. T. Chen, *Phys. Rev. B* **69**, 085107 (2004).

⁵¹A. O. Sboychakov, K. I. Kugel, A. L. Rakhmanov, and D. I. Khomskii, *Phys. Rev. B* **80**, 024423 (2009).

⁵²H. Fujishiro, T. Naito, S. Ogawa, N. Yoshida, K. Nitta, J. Hejtmánek, K. Knížek, and Z. Jirák, *J. Phys. Soc. Jpn.* **81**, 064709 (2012).

⁵³A. Podlesnyak, M. Russina, A. Furrer, A. Alfonsov, E. Vavilova, V. Kataev, B. Büchner, Th. Strässle, E. Pomjakushina, K. Conder, and D. I. Khomskii, *Phys. Rev. Lett.* **101**, 247603 (2008).

⁵⁴R. Fehrenbacher and T. M. Rice, *Phys. Rev. Lett.* **70**, 3471 (1993).